Filtering Microstrip Patch Antenna Design Using Coupling Matrix Approach for ISM Applications

Original Scientific Paper

Kharmana Ramazan Ahmad
Department of Physics, College of Education, Salahaddin University-Erbil,
Erbil, Kurdistan Region, Iraq
kharmana.ahmed@su.edu.krd

Rashad H. Mahmud*
Department of Physics, College of Education, Salahaddin University-Erbil,
Erbil, Kurdistan Region, Iraq
Mechatronic Engineering, Faculty of Engineering, Tishk International University,
Erbil, Iraq
rashad.mahmud@su.edu.krd
*Corresponding author

Abstract *– This paper presents a novel design approach for a filtering microstrip patch antenna inspired by a bandpass filter (BPF). It is based on the coupling matrix approach, where the magnitudes of the matrix elements are utilized to extract the physical dimensions. Two rectangular microstrip patch resonators (RMPRs) are directly coupled via an air-gap to realize a second-order BPF and a filtering microstrip patch antenna. For the BPF, a 50-Ω microstrip feedline is employed at the input/output ports and extended into the center of the RMPRs to ensure strong impedance matching within the passband of interest. For the filtering antenna, the output feedline port is removed, and the second RMPR is modified to obtain the required radiation quality factor and provide radiation within the passband frequency range. To validate the proposed approach, both designs are fabricated and experimentally tested, showing excellent agreement with the simulation results. The measured 10-dB fractional bandwidth (FBW), passband peak gain, and total efficiency are 4.05%, 6.0 dBi, and 74.0%, respectively. These results demonstrate that the proposed designs offer a compact size, high gain, and high efficiency, making them promising candidates for ISM band applications.*

Keywords: *Bandpass filter, cavity resonators, coupling matrix, filtering antenna, microstrip patch*

Received: August 1, 2025; Received in revised form: September 28, 2025; Accepted: October 30, 2025

1. INTRODUCTION

Microstrip patch antennas are well-suited for industrial scientific medical (ISM) systems not only due to their compact size, light-weight and low profile characteristics [1-5], but also because they can be seamlessly integrated with other system components [6, 7]. This direct integration eliminates the need for additional matching circuits and realizes system miniaturization. However, conventional microstrip patch antennas suffer from their inherent narrow bandwidth performances, restricting their applications in wideband and ISM technologies [3, 8]. To remedy this limitation, filtering microstrip patch antennas have been introduced, combining both radiation and filtering functionalities into a single integrated component [9]. This integration offers miniaturizing the front-end size, eliminating the insertion loss caused by separate BPF filters, and simplifying the front-end system architecture [10]. Additionally, the bandwidth of filtering microstrip patch antennas can be broadened by appropriately tuning the resonant frequencies of the coupled-resonators within the antenna radiating structure.

Various design approaches have been investigated to implement filtering functionalities in microstrip patch antenna. Among these is the coupled-resonator filter synthesis approach [9, 11], where the patch serves as the last coupled-resonator in the filter while also acting as a radiator. Techniques such as the use of metal strips [12], shorting pins [13], stub-loaded resonators [14], coupling structures [15-17], and slot-loaded patches [18, 19] have been explored to improve the frequency selectivity and widen the bandwidth of filtering microstrip antennas [12-19]. Modified patch shapes, including U-shaped [20, 21], T-shaped [6], bow tie-shaped

[22], square ring [23], cross-shaped [24], ground slots [25], and inverted-F configuration [26] have also been employed. In addition, other enhancement techniques such as defected ground structure (DGS) [27, 28], and various feedline structures like fork-shaped [29], split-merge [30], and dual baluns [11] have been introduced to realize desired filtering characteristics to microstrip patch antennas. Equivalent circuit models based on the lumped LC elements have also been proposed for slot-loaded patch designs [31, 32].

Despite these advances in filtering patch antenna designs, many of the existing techniques require extra circuit structure, which increases the overall size and design complexity. To address this issue, we propose a new filtering microstrip patch antenna design approach based on the coupling matrix approach, in which no additional coupling structures or circuits are required to realize filtering functionality. In section 2, the approach is applied to a second-order BPF using rectangular patch resonators, where matrix elements are interpreted into physical dimensions. In Section 3, the filter's output port is removed, and the second-coupled patch is modified to achieve the required radiation quality factor (Q_r) while maintaining its dual functionality of frequency selectivity and radiation. Section 4 presents the fabrication and measurement of two prototypes to validate the proposed method. Finally, the conclusions are summarized in section 5.

2. BPF DESIGN

Fig. 1 illustrates the topology and corresponding physical layout of a second-order microstrip BPF with an all-resonator configuration. The substrate material chosen is Rogers RO4350B™, which has a relative permittivity (ε_r) of 3.48, thickness (h) of 1.524 mm, and a loss tangent of 0.0037. The patch and ground plane are both 0.035 mm thick, and made using copper with a conductivity of 5.8×10^7 S/m. A two-pole Chebyshev low-pass prototype is chosen with a FBW of 3.0% at a center frequency (f_0) of 3.0 GHz, and a passband ripple of 0.0432 dB are chosen for the design. The simulated performance is obtained using the computer simulation technology (CST) simulator.

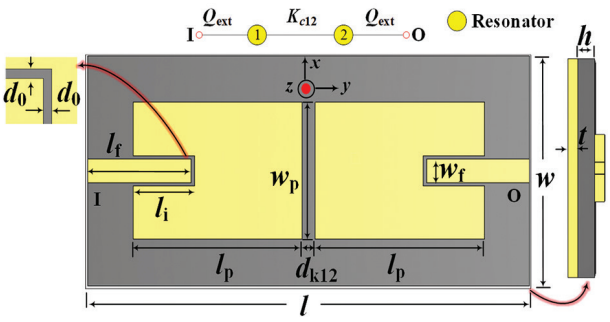

Fig. 1. Topology and physical layout of the second-order BPF. Dimensions in mm are: l=67.09, w=33.68, l_f=16.25, w_f=3.43, l_i=9.50, l_p=26.20, w_p=20, d_0=0.20, h=1.524, t=0.035, d_{k12}=0.8.

2.1. COUPLING MATRIX

The scaled external quality factors ($q_{ext1}= q_{ext2}$), scaled coupling coefficient between direct coupled-resonators ($m_{12}= m_{21}$), and reflection coefficient (S_{11}) of the BPF can be calculated using the relations [33]:

$$q_{\text{ext1}} = g_0 g_1 \tag{1}$$

$$m_{1,2} = \frac{1}{\sqrt{g_1 g_2}} \tag{2}$$

$$S_{11} = \pm\left(1 - \frac{2}{q_{\text{ext1}}}\right).[A]^{-1}_{11} \tag{3}$$

$$S_{21} = 2\frac{1}{\sqrt{q_{\text{ext1}} q_{\text{ext2}}}}.[A]^{-1}_{11} \tag{4}$$

$$[A] = \begin{bmatrix} \frac{1}{q_{\text{ext1}}} & 0 \\ 0 & \frac{1}{q_{\text{ext2}}} \end{bmatrix} + j\frac{1}{FBW}\left(\frac{\omega}{\omega_0} - \frac{\omega_0}{\omega}\right)\begin{bmatrix} 1 & 0 \\ 0 & 1 \end{bmatrix} - j\begin{bmatrix} 0 & m_{12} \\ m_{21} & 0 \end{bmatrix} \tag{5}$$

Here g_0, g_1, g_2 are the low-pass prototype parameters, and their values for the given topology can be found in [33] as: g_0=1.0, g_1=0.6648, g_2=0.5445. The ω and ω_0 are the center and passband edge angular frequencies, respectively. The un-scaled external quality factor Q_{ext1} (Q_{ext1}=$qext_1/FBW$) and un-scaled coupling coefficient M_{12} ($M_{12}= m_{12}\,FBW$) are calculated, using the aforementioned relations, and are found to be 22.16 and 0.049, respectively.

2.2. PARAMETRIC EXTRACTIONS

This section describes the extraction of the physical dimensions (d_0, d_{k12}) of the BPF illustrated in Fig. 1 using the calculated values of Q_{ext} and M_{12}. The dimensions of the patches (l_p, w_p) and feedlines (l_f, w_f) are calculated, utilizing the transmission line equations given in [34], and are provided in the caption of Fig. 1. To extract the dimension d0, the set up shown in Fig. 2a is employed. In this configuration, resonator 1 is weakly coupled to the output port (i.e. h_0 is large), while the dimension d_0 is tuned to achieve the desired Q_{ext} value from the S21 response as illustrated in Fig. 2b using the relation [9]:

$$Q_{\text{ext}} = \frac{f_0}{\Delta f_{3dB}} \tag{3}$$

As shown in Fig. 2c, the value of Q_{ext} increases with an increase in the d_0 dimension. The desired value of Q_{ext}=22.16 is obtained when d_0= 0.20 mm.

Fig. 3a shows the physical setup used to extract the (M_{12}) between resonators 1 and 2. In this configuration, both resonators are weakly coupled to the input and output ports. The gap dk_{12} is adjusted to achieve the desired M_{12} value from the S_{21} response shown in Fig. 3b using the relation [9]:

$$M_{12} = \frac{f_2^2 - f_1^2}{f_2^2 + f_1^2} \tag{4}$$

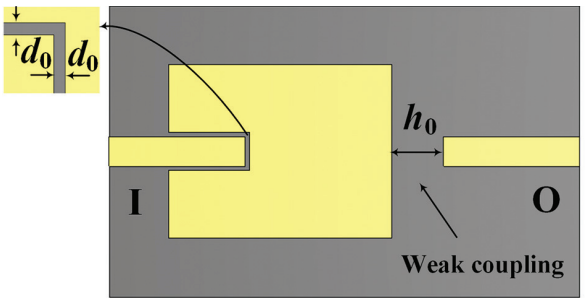

(a)

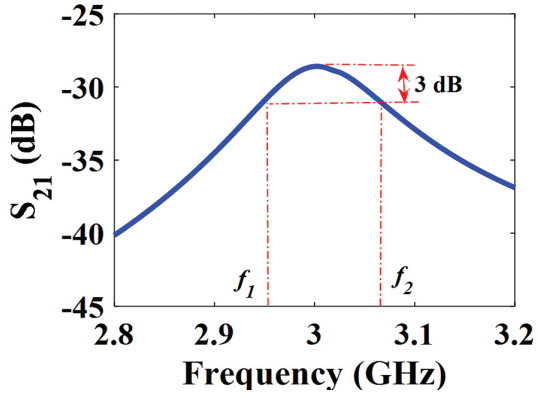

(b)

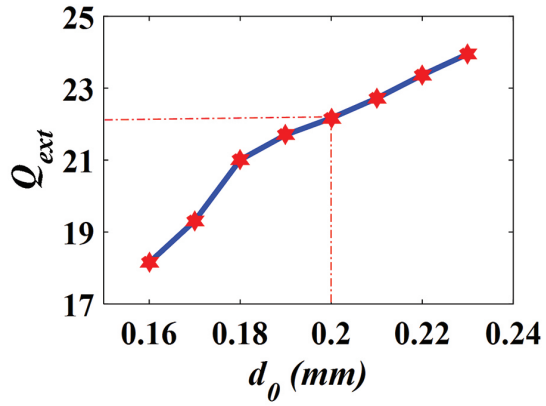

(c)

Fig. 2. (**a**) Physical layout set up for d_0 extraction, (**b**) its S_{21} response, and (c) variation of Q_{ext} versus d_0

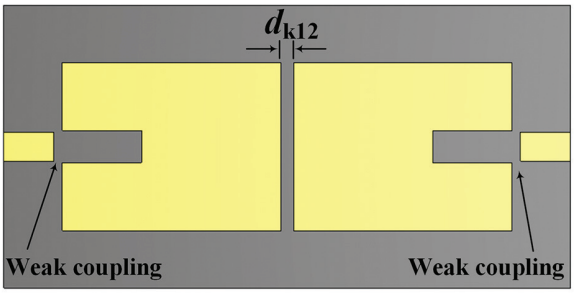

(a)

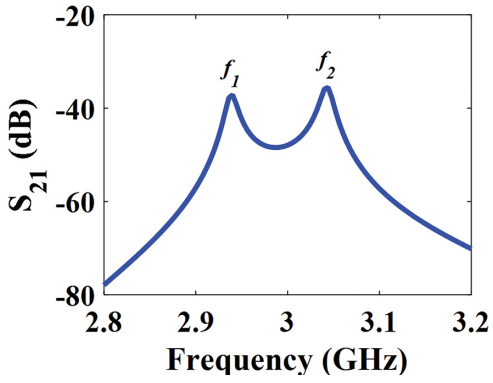

(b)

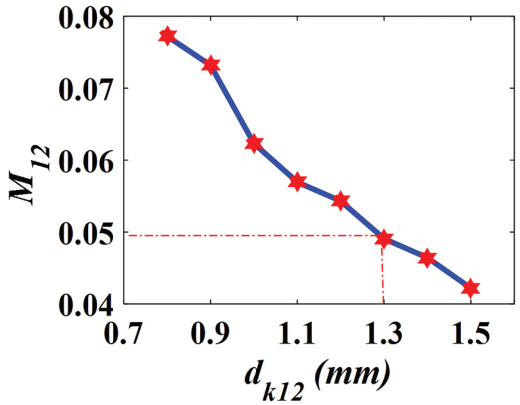

(c)

Fig. 3. (**a**) Physical layout set up for dk_{12} extraction, (**b**) S_{21} response, and (c) variation of M_{12} versus dk_{12}

Here, the f_1 and f_2 represent the split resonant frequencies of resonators 1 and 2, respectively. As illustrated in Fig. 3c, the value of M_{12} reduces with an increase in the gap d_{k12}. The required value of M_{12}=0.049 is achieved when d_{k12}=1.28 mm.

The dimensions d_0 and d_{k12} extracted above are considered as their initial values, and optimization is performed in CST to achieve the desired results. Fig. 4 shows the S_{11} and S_{21} responses of the proposed BPF, obtained both from the coupling matrix equations 4 and 5 and from CST simulator. As shown, the simulated and calculated results are in excellent agreement within the operating frequency band. The designed filter achieves a FBW of 3.0% centered at 3.0 GHz, with an insertion loss of 0.8 dB over the passband. The filter also exhibits a selectivity better than 30 dB in both the lower and upper stopbands.

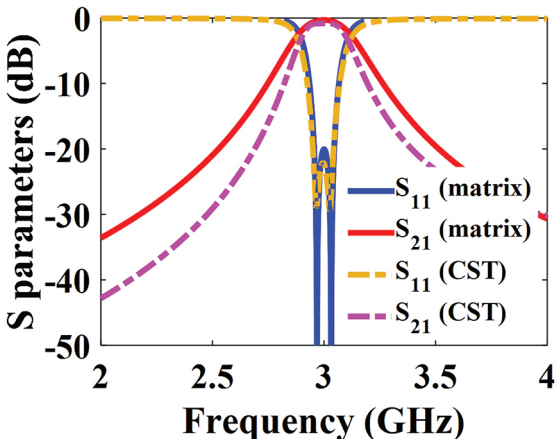

Fig. 4. Simulated and calculated S_{11} and S_{21} responses of the proposed second-order BPF.

3. FILTERING ANTENNA DESIGN

The topology and its corresponding physical layout of the proposed second-order filtering microstrip patch antenna is shown in Fig. 5. Unlike the BPF, where resonator 2 is coupled to an electrical output port, the filtering microstrip patch antenna connects resonator 2 (so-called *radiating-radiator*) to free space, enabling radiation at center frequency of 3.0 GHz. To keep its filtering functionality function alongside its radiation role within the bandwidth of interest, the dimensions of the *radiating resonator* and the coupling gap (d_{s12}) between resonators 1 and *radiating resonator* must be carefully optimized. Specifically, the Q_r value of the *radiating resonator* must match the Q_{ext} at the input port (i.e. Q_r=Q_{ext}=22.16) to ensure balanced power distribution and proper filtering performance.

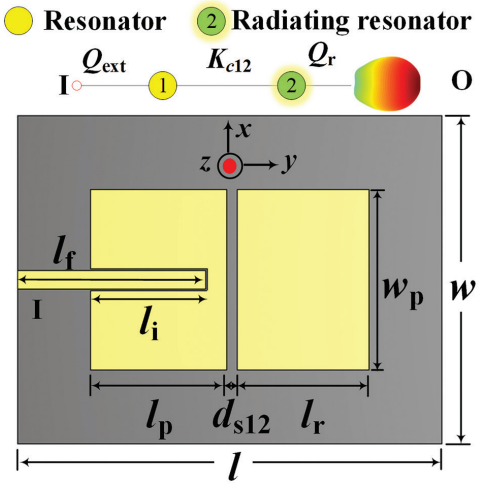

Fig. 5. Topology and physical layout of the second-order filtering antenna. Dimensions in mm are: l=80.28, w=61.78, l_f=35.59, w_f=3.43, l_i=22.0, l_p=25.70, l_r=24.90, w_p=34, d_0=0.30, h=1.524, t=0.035, d_{s12}=1.9

3.1. PARAMETRIC EXTRACTIONS

The configuration shown in Fig. 6a is utilized to extract the Q_r of the *radiating resonator*, following the procedure outlined in section 2.2. In this setup, the *radiating resonator* is very weakly coupled to the input and output ports. From the simulated S_{21} response shown in Fig 6b, the required Q_r is determined using the Δf_{3dB} magnitude and applying into equation 3. To minimize the number of design variables, only the length of the *radiating resonator* (l_r) is adjusted to control the Q_r value. As shown in Fig. 6b, the Δf_3dB value decreases (Q_r increases) with an increase in l_r dimension.

Fig. 7a shows the physical setup used to extract the coupling gap (d_{s12}) between resonator 1 and the *radiating resonator*. By following the extraction method described in Section 2.2 and inserting the split resonance frequencies of resonator 1 (f_1) and *radiating resonator* (f_r) obtained from the simulated S_{21} response shown in Fig. 7b into equation 4, the required M_{12} value can be determined by adjusting d_{s12} dimension.

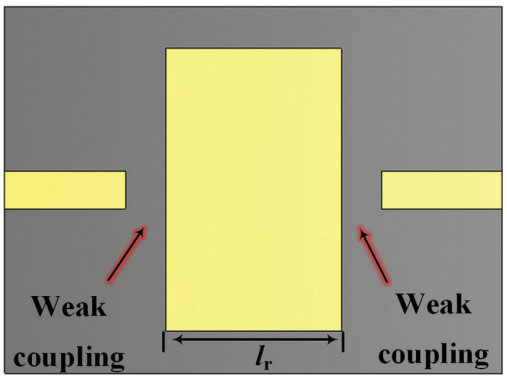

(a)

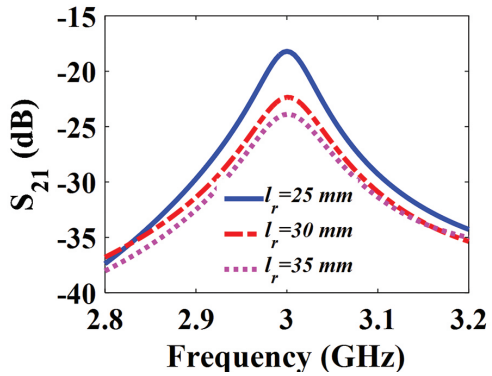

(b)

Fig. 6. (a) Physical layout set up for Q_r extraction, (b) its S_{21} response

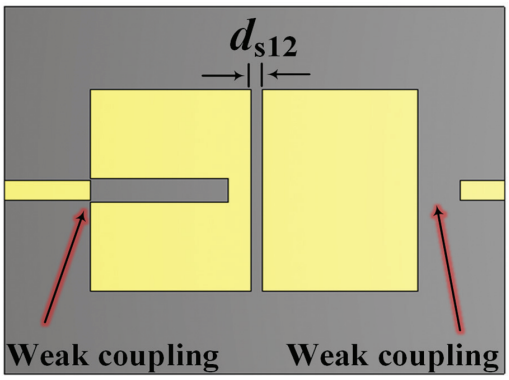

(a)

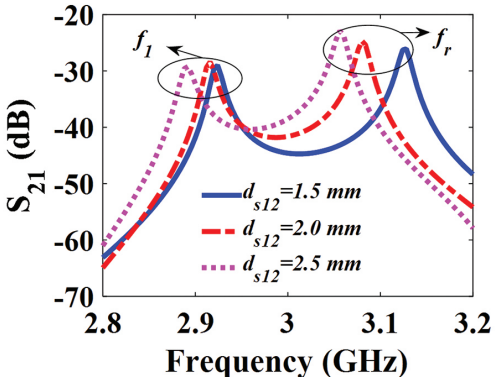

(b)

Fig. 7. (**a**) Physical layout set up for d_{s12} extraction, and (**b**) S_{21} response

3.2. SIMULATED RESULTS AND COMPARISON

Fig. 8 compares the simulated responses of the proposed second-order BPF and the second-order filtering antenna. The S_{11} responses of both designs show excellent agreement across the operating frequency band. Furthermore, the normalized realized gain of the filtering microstrip patch antenna exhibits a filter-like S_{21} response within the passband of interest. Discrepancies observed at the lower and upper stop bands are attributed to unexpected radiation from patch structures.

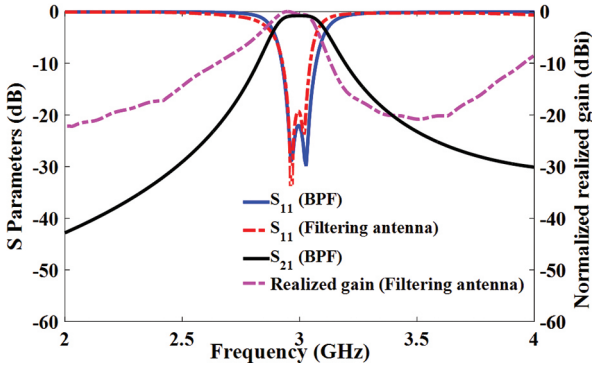

Fig. 8. Simulated S_{11}, S_{21} and realized gain of the proposed BPF and filtering antenna

To demonstrate the advantages of the proposed filtering antenna, its performance is compared with that of a conventional rectangular microstrip patch antenna, as shown in Fig. 9a. The dimensions of the patch are calculated based on the cavity model theory [34-36], and are provided in the caption of Fig. 9. For consistency, the materials used in the ground plane, patch, and substrate of the conventional patch antenna are the same as those employed in the proposed filtering antenna. The simulated S_{11} and realized gain of both conventional and proposed filtering patch antennas are shown in Fig. 9b. The proposed filtering microstrip patch antenna exhibits several improvements over the conventional one. For instance, within the passband, it provides a 1.0 dBi higher realized gain. Also, it exhibits more than 20 dB selectivity at both the lower and upper frequency edges.

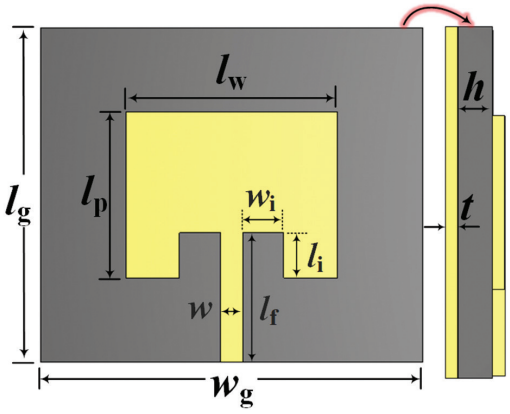

(a)

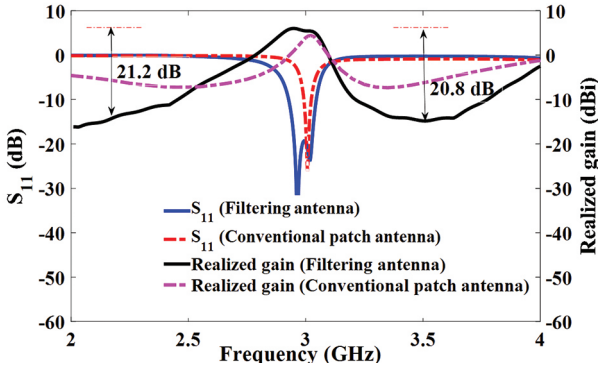

(b)

Fig. 9. (**a**) Layout of a conventional rectangular microstrip patch antenna. (**b**) Simulated S_{11} and realized gain responses of proposed filtering microstrip patch antenna and conventional rectangular patch antenna. Dimensions in mm are: l_g=54.11, w_g=60.20, l_i=7.20, w_i=6.50, l_f=20.60, w=3.43, l_w=33.40, l_p=26.33.

This enhanced selectivity can potentially eliminate the need for an additional BPF in the front-end of the wireless system, thereby reducing mismatch and insertion losses. The 10-dB FBW of the filtering microstrip patch antenna is 3.97%, which is approximately three times wider than that of the conventional patch antenna.

4. FABRICATIONS AND MEASUREMENTS

Fig. 10a shows the actual photograph of the proposed BPF under test. The scattering parameters were measured using an Agilent Vector Network Analyzer (VNA). Fig. 10b compares the measured and simulated S_{11} and S_{21} responses. The measured 10-dB FBW is 3.10 %, which is slightly larger than the simulated value of 3.0 %. The measured insertion loss across the passband is 1.10 dB, compared to 0.80 dB in simulation. The 3-dB passband bandwidths from the measurement and simulation are 0.10 GHz and 0.22 GHz, respectively. The measured start stop band rejection is below 20 dB, while the upper stop band reaches approximately 35 dB. The measured center frequency is 2.9 GHz, exhibiting a downward shift of 0.1 GHz from the simulated 3.0 GHz. These discrepancies are mainly attributed to fabrication tolerances, SMA connector effects, and dielectric loss.

Fig. 11a shows the manufactured filtering antenna. The S_{11} response was measured using the VNA. Radiation patterns were measured in an anechoic chamber room using a wide bandwidth reference horn antenna positioned in the far-field region. As shown in Fig. 11b, the measured S_{11} and realized gain match the simulated results across the operating frequency band. The measured 10-dB FBW is 4.05%, which is slightly wider than the simulated value of 3.97%. The realized gain across the passband is relatively flat, with a fluctuation of approximately 0.68 dBi. The measured peak gain is 6.0 dBi at 2.95 GHz, and the 3-dB gain bandwidth is 7.0%. Re-

alized gain selectivity of around 20 dB is observed at both lower and upper frequency bands. Fig. 12 a shows the measured total efficiency, calculated as the ratio of measured realized gain to the simulated directivity. It is exceeding 74% within the passband, slightly lower than the simulated 81.0%. The efficiency degradation is attributed to the frequency-dependent variation of the substrate loss tangent and the unexpected radiation from the microstrip coupling edges. As depicted in Figs. 12 b and 12 c, the measured E-plane and H-plane radiation patterns align well with the simulations. The slight discrepancies in the backside radiation are likely due to the presence of the SMA connector and the transmission cable during the measurement.

Table 1 compares the measured performance of the proposed filtering microstrip patch antenna with related designs reported in the literature. Among the cited works, only [37] and the present design achieve filtering characteristics without requiring additional circuitry. The filtering antennas presented in [30, 32] demonstrate relatively high gains of 10 dBi and 7.55 dBi, respectively; however, their large physical dimensions and moderate FBW reduce their suitability for ISM band applications due to occupying larger area and limiting the operating frequency range. The designs in [37, 38] exhibit strong frequency selectivity at both lower and upper stop bands, but the low realized gains are as their main drawbacks. Antennas in [39] and [40] provided large bandwidths, but their bulky size and low gain are their main drawbacks. In contrast, the proposed filtering microstrip patch antenna offers a competitive profile, combining compact size, moderate bandwidth, high gain, and high efficiency. These features are extremely demanded for ISM band applications.

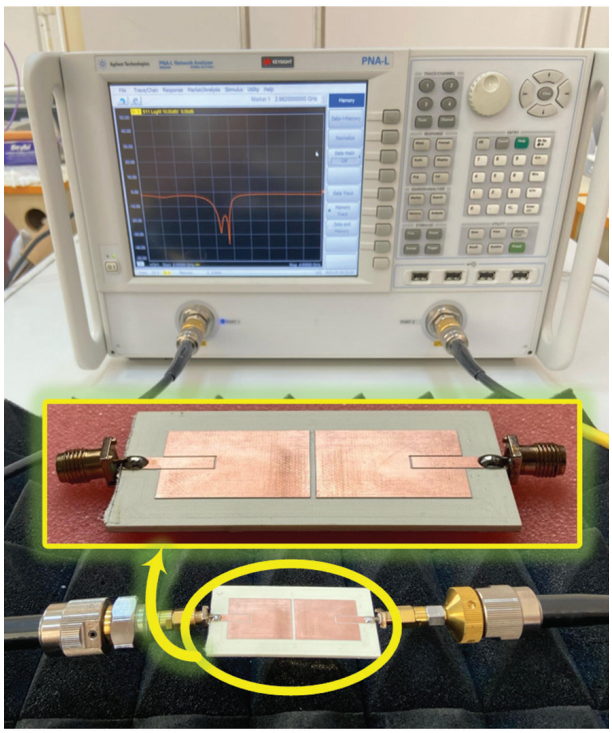

(a)

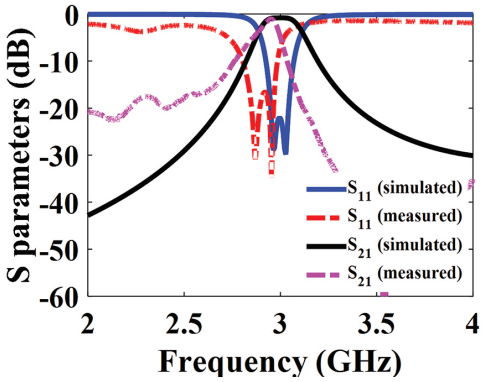

(b)

Fig. 10. (**a**) Actual BPF under test, and (**b**) measured S11 and S21 performances of BPF compared with simulated ones

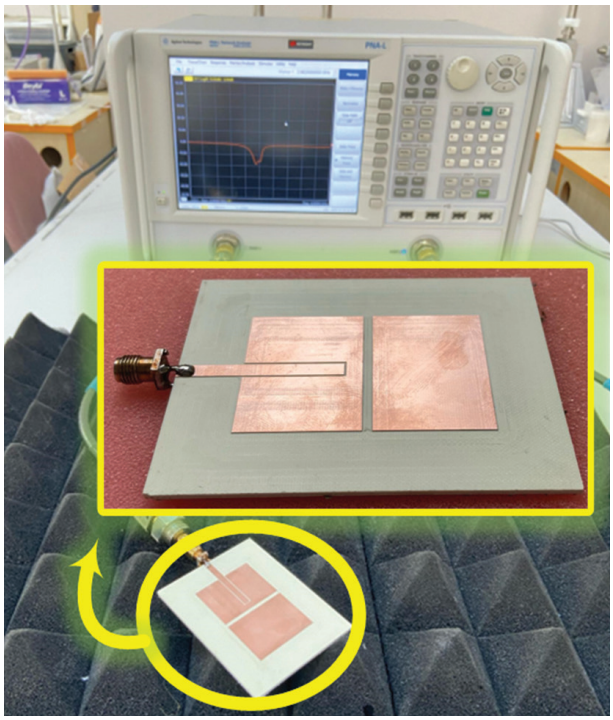

(a)

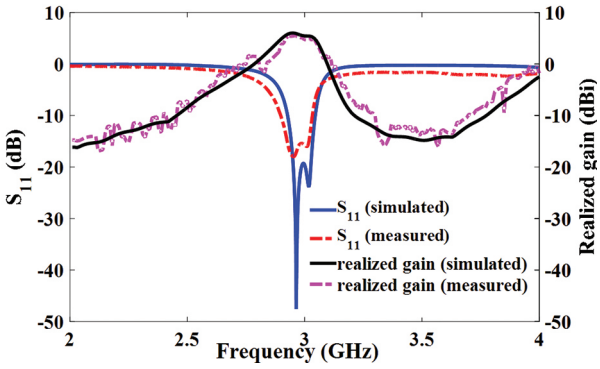

(b)

Fig. 11. (**a**) Actual filtering microstrip patch antenna under test, and (**b**) measured S_{11} and realized gain performances of filtering microstrip patch antenna compared with simulated ones

Table 1. Performance of the proposed filtering microstrip patch antenna compared with some related works

Refs.	Antenna types	f0 (GHz)	Size (λ_0^3)	10-dB FBW (%)	Peak gain (dBi)	Lower/Upper Rejection level (dB)	Total Efficiency (%)	extra circuit or structure
[6]	H-shaped patch	2.45	0.361×0.426×0.013	< 4.0	6.0	-40.1/-39	> 90	Yes
[30]	Slot-loaded patch	9.8	1.96 ×1.50×0.026	5.1	10	NA	> 90	Yes
[32]	Rectangular patch	10	0.94×0.94×0.017	3.7	7.55	17/17	NA	Yes
[37]	Rectangular patch	2.0	NA	2.03	5.0	15/23	NA	No
[38]	U-shaped split ring	3.6	18.33×11.11×0.27	33.4	4.5	> 20	NA	Yes
[39]	Monopole	3.8	0.31×0.83×0.011	62.9	3.0-3.5	NA	NA	Yes
[40]	U-shaped parasite patch	5.5	0.94×0.94×0.066	26.38	7.98	11	> 92	Yes
This work	Rectangular Patch	3.0	0.67 ×0.33×0.0152	4.05	6.0	21.2/20.5	74.0	No

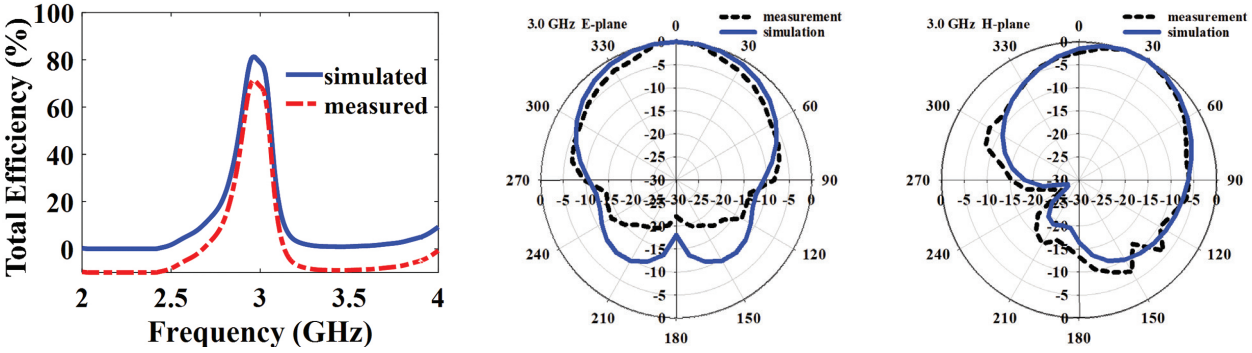

(a) (b) (c)

Fig. 12. (**a**) measured total efficiency compared with simulation. (**b**) measured E-plane, and (**c**) H-plane patterns compared with simulated ones.

5. CONCLUSIONS

This paper presented a novel design approach for a filtering microstrip patch antenna based on the coupling matrix approach. The matrix elements were utilized to extract the physical dimensions of the antenna and to embed filtering characteristics without the need for additional physical structures. Two prototypes were fabricated, and the measured results showed good agreement with the simulated predictions, validating the proposed coupling matrix design approach. The proposed filtering microstrip patch antenna demonstrated competitive performance and is a promising candidate for ISM band applications.

ACKNOWLEDGEMENT

The authors would like to thank the EDT Research Center at the School of Engineering, University of Birmingham, and Iskenderun Technical University for providing technical support for antenna performance measurements. This work was supported by Salahaddin University-Erbil.

REFERENCES:

[1] C. Chen, "A single-layer single-patch dual-polarized high-gain cross-shaped microstrip patch antenna", IEEE Antennas and Wireless Propagation Letters, Vol. 22, No. 10, 2023, pp. 2417-2421.

[2] R. H. Mahmud, "Terahertz microstrip patch antennas for the surveillance applications", Kurdistan Journal of Applied Research, Vol. 5, No. 1, 2020, pp. 16-27.

[3] G. Mansour, E. Nugoolcharoenlap, R. H. Mahmud, T. Tippo, P. Akkaraekthalin, D. Torrungrueng, "Circularly Polarized Elliptical Patch Array Antennas for GPS", Proceedings of the Research, Invention, and Innovation Congress: Innovation Electricals and Electronics, Bankok, Tahiland, 1-3 September 2021, pp. 92-96.

[4] R. Y. Khattak, Q. Z. Ahmed, S. Shoaib, P. I. Lazaridis, T. T. Alade, "Recent advances in antennas for biotelemetry and healthcare applications", IEEE Open Journal of Antennas and Propagation, Vol. 5, No. 6, 2024, pp. 1499-1522.

[5] C. Liu, Y.-X. Guo, S. Xiao, "Capacitively loaded circularly polarized implantable patch antenna for ISM band biomedical applications", IEEE transactions on antennas and propagation, Vol. 62, No. 5, 2014, pp. 2407-2417.

[6] Z. Zheng, D. Li, X. Tand, M. Wang, Y. Deng, "Compact low-profile differential filtering microstrip patch antenna with high selectivity and deep rejection using single-layer substrate", IEEE Access, Vol. 9, No. 1, 2021, pp. 76047-76055.

[7] H. Jin, G. Q. Luo, W. Che, K.-S. Chin, Y. Pan, Y. Yu, "Vertically-integrated differential filtering patch antenna excited by a balun bandpass filter", IET Microwaves, Antennas & Propagation, Vol. 13, No. 3, 2019, pp. 300-304.

[8] L. Ma, Z. Shao, J. Lai, C. Gu, J. Mao, "Bandwidth enhancement of H-plane MIMO patch antennas in integrated sensing and communication applications", IEEE Open Journal of Antennas and Propagation, Vol. 5, No. 1, 2023, pp. 90-103.

[9] R. H. Mahmud, H. N. Awl, Y. I. Abdulkarim, M. Karaaslan, M. J. Lancaster, "Filtering two-element waveguide antenna array based on solely resonators", AEU-International Journal of Electronics and Communications, Vol. 121, 2020, p. 153232.

[10] R. H. Mahmud, M. J. Lancaster, "High-gain and wide-bandwidth filtering planar antenna array-based solely on resonators", IEEE Transactions on Antennas and Propagation, Vol. 65, No. 5, 2017, pp. 2367-2375.

[11] C.-K. Lin, S.-J. Chung, "A filtering microstrip antenna array", IEEE transactions on microwave theory and techniques, Vol. 59, No. 11, 2011, pp. 2856-2863.

[12] J. Guo, Y. Chen, D. Yang, K. Sun, J. Pan, S. Liu, "Design of wideband filtering patch antenna array with high aperture efficiency and good filtering performance", IEEE Transactions on Antennas and Propagation, Vol. 72, No. 1, 2023, pp. 974-979.

[13] D. Yang, H. Zhai, C. Guo, H. Li, "A compact single-layer wideband microstrip antenna with filtering performance", IEEE Antennas and Wireless Propagation Letters, Vol. 19, No. 5, 2020, pp. 801-805.

[14] H.-Y. Xie, B. Wu, L.-W. Song, Y.-L. Xin, J.-Z. Chen, T. Su, "High-gain third-order filtering patch antenna array with two radiation nulls using cross-radiation", IEEE Transactions on Circuits and Systems II: Express Briefs, Vol. 70, No. 11, 2023, pp. 4053-4057.

[15] J. Liang, D. Wang, Z. Qi, Y. Gao, Q. Wei, "Design of A Microstrip Filtering Antenna without Extra Circuits and Its Application in Orbital Angular Momentum (OAM) Filtering Antenna", Progress In Electromagnetics Research Letters, Vol. 11, 2024, pp. 1-8.

[16] W. Yang, Y. Zhang, W. Che, M. Xun, Q. Xue, G. Shen, "A simple, compact filtering patch antenna based on mode analysis with wide out-of-band suppression", IEEE Transactions on Antennas and Propagation, Vol. 67, No. 10, 2019, pp. 6244-6253.

[17] C. Chen, "A compact wideband endfire filtering antenna inspired by a uniplanar microstrip antenna", IEEE Antennas and Wireless Propagation Letters, Vol. 21, No. 4, 2022, pp. 853-857.

[18] Q. Liu, L. Zhu, "A compact wideband filtering antenna on slots-loaded square patch radiator under triple resonant modes", IEEE Transactions on Antennas and Propagation, Vol. 70, No. 10, 2022, pp. 9882-9887.

[19] C. Chen, "A wideband coplanar L-probe-fed slot-loaded rectangular filtering microstrip patch antenna with high selectivity", IEEE Antennas and Wireless Propagation Letters, Vol. 21, No. 6, 2022, pp. 1134-1138.

[20] H. Chang, M. Liu, D. Lin, J. Wang, "A compact single layer filtering antenna with DGS for 5.1 GHz application", Progress In Electromagnetics Research Letters, Vol. 107, 2022, pp. 1-7.

[21] L. Li, G. Liu, "A differential microstrip antenna with filtering response", IEEE Antennas and Wireless Propagation Letters, Vo. 1, No. 5, 2016, pp. 1983-1986.

[22] B. Maity, S. K. Nayak, "Compact bowtie-shaped microstrip patch antennas with low cross-polarization and wideband harmonic suppression", AEU-International Journal of Electronics and Communications, Vol. 168, 2023, p. 154699.

[23] G. Liu, P. F. Hu, G. D. Su, Y. M. Pan, "Bandwidth and gain enhancement of a single-layer filtering patch antenna using reshaped TM mode", IEEE Antennas and Wireless Propagation Letters, Vol. 23, No. 1, 2023, pp. 314-318.

[24] R. Wu, W. Liu, Z. Jiang, W. Kuang, "A Low-Profile Broadband Filtering Antenna and Its Array for 5G Applications", IEEE Antennas and Wireless Propagation Letters, Vol. 23, No. 10, 2024, pp. 29220-2924.

[25] X. Lin, W. Liu, Z. Jiang, W. Kuang, "Broadband Filtering Circularly Polarized Patch Antenna Based on Ground Slot and Coupling Stub", IEEE Open Journal of Antennas and Propagation, 2025. (in press)

[26] M. Li, S. Tian, M.-C. Tang, L. Zhu, "A compact low-profile hybrid-mode patch antenna with intrinsically combined self-decoupling and filtering properties", IEEE Transactions on Antennas and Propagation, Vol. 70, No. 2, 2021, pp. 1511-1516.

[27] X. Chen, Q. Zhuge, G. Han, R. Ma, J. Su, Wenmei Zhang, "A wideband harmonic suppression filtering antenna with multiple radiation nulls", Progress In Electromagnetics Research Letters, Vol. 112, 2023, pp. 15-23.

[28] H. Gui, Z. Wang, W. Nie, M. Yang, M. Wang, "Design of a Compact Wideband Filtering Antenna with High Frequency Selectivity", Progress In Electromagnetics Research M, Vol. 131, 2025, pp. 27-35.

[29] S. Liu, Z. Wang, Y. Dong, "A compact filtering patch antenna with high suppression level and its CP application", IEEE Antennas and Wireless Propagation Letters, Vol. 22, No. 4, 2022, pp. 769-773.

[30] S. Ramkumar, M. Saravanan, S. Saran, S. S. Varshith, "A high gain filtenna with radiation nulls using a novel split-merge feed line on a slot-loaded rectangular patch for X-band RADAR application", AEU-International Journal of Electronics and Communications, Vol. 196, 2025, p. 155789.

[31] N. García-Alcaide, A. Fernandez-Prieto, R. R. Boix, V. Losada, J. Martel, F. Medina, "Design of broadband aperture-coupled stacked microstrip antennas using second-order filter theory", IEEE Transactions on Antennas and Propagation, Vol. 70, No. 7, 2022, pp. 5345-5356.

[32] Ji, S., Y. Dong, Y. Fan, "Bandpass filter prototype inspired filtering patch antenna/array", IEEE Transactions on Antennas and Propagation, Vol. 70, No. 5, 2021, pp. 3297-3307.

[33] J.-S. G. Hong, M. J. Lancaster, "Microstrip filters for RF/microwave applications", 1st Edition, John Wiley & Sons, 2004.

[34] C. A. Balanis, "Antenna theory: analysis and design", 4th Edition, John Wiley & Sons, 2016.

[35] S. O. Hasan, S. K. Ezzulddin, O. S. Hammd, R. H. Mahmud, "Design and performance analysis of rectangular microstrip patch antennas using different feeding techniques for 5G applications", International Journal of Electrical and Computer Engineering Systems, Vol. 14, No. 8, 2023, pp. 833-841.

[36] S. O. Hasanet, S. K. Ezzulddin, R. H. Mahmud, M. J. Ahmed, "Design and simulation of microstrip antenna array operating at S-band for wireless communication system", International Journal of Electrical and Computer Engineering Systems, Vol. 14, No. 5, 2023, pp. 497-506.

[37] G. Mansour, M. J. Lancaster, P. S. Hall, P. Gardner, E. Nugoolcharoenlap, "Design of filtering microstrip antenna using filter synthesis approach", Progress In Electromagnetics Research, Vol. 145, 2014, pp. 59-67.

[38] X. Yang, L. Cui, Z. Ding, Z. Zhang, "A 5G filtering antenna simultaneously featuring high selectivity and band notch", AEU-International Journal of Electronics and Communications, Vol. 153, 2022, p. 154299.

[39] M. Ribó, M. Cabedo-Fabrés, L. Pradell, S. Blanch, M. Ferrando-Bataller, "Multimodal planar monopole filtenna for 5G applications", AEU-International Journal of Electronics and Communications, Vol. 180, 2024, p. 155338.

[40] W. Huang, P. Wang, S. Hou, "Wideband filtering antenna loading U-shaped parasitic patches based on characteristic mode analysis", Scientific Reports, Vol. 15, No. 1, 2025.